



Sol–Gel Derived Organic and Inorganic Hybrid Materials for Photonic Applications: Contribution to the Correlation Between the Material Structure and the Transmission in the Near Infrared Region

M. OUBAHA

Laboratoire Des Verres, UMR 5587, Université de Montpellier II, Place Eugène Bataillon, Montpellier Cedex 5 34090, France; Centre d'Electronique et de Micro-Optoélectronique de Montpellier, UMR 5507, Université de Montpellier II Place Eugène Bataillon, Montpellier Cedex 5 34090, France; Laboratoire des Matériaux Inorganiques CNRS UMR 6002, Université Blaise Pascal and ENSCCF, 24 Avenue des Landais, Aubière 63177, France

P. ETIENNE AND S. CALAS

Laboratoire Des Verres, UMR 5587, Université de Montpellier II, Place Eugène Bataillon, Montpellier Cedex 5 34090, France

P. COUDRAY

Centre d'Electronique et de Micro-Optoélectronique de Montpellier, UMR 5507, Université de Montpellier II Place Eugène Bataillon, Montpellier Cedex 5 34090, France

J.M. NEDELEC

Laboratoire des Matériaux Inorganiques CNRS UMR 6002, Université Blaise Pascal and ENSCCF, 24 Avenue des Landais, Aubière 63177, France

Y. MOREAU

Centre d'Electronique et de Micro-Optoélectronique de Montpellier, UMR 5507, Université de Montpellier II Place Eugène Bataillon, Montpellier Cedex 5 34090, France

Received February 23, 2004; Accepted July 1, 2004

Abstract. A promising way of fabricating integrated optics components is based on the sol–gel synthesis and photocuring of organic-inorganic hybrid materials. However, the main factor limiting the development of passive devices is the propagation losses. Moreover, the possibility to compensate these attenuations by optical amplification is competed with the multiphonon relaxation associated to the presence of OH groups. To our knowledge, OH groups were always shown as the main responsible for attenuation at the telecommunication wavelengths, namely at 1310 and 1550 nm, although the matrix is composed of organic species which can contribute to absorptions in this spectral range. This paper deals with spectroscopic and optical characterizations of a well established organic and inorganic hybrid material in order to determine the contribution of each molecular groups to the attenuation at the aforementioned wavelengths.

1. Introduction

The large expansion of telecommunication networks and the exponential growth of internet have led to the necessity to both improve performances of data transport and to create new devices such as power splitters, couplings and wavelength demultiplexer/multiplexer.

In the last ten years, organically modified silicates ($R'Si(OR)_{4-x}$) prepared by the sol-gel process have demonstrated adequate value for the fabrication of photonic devices for the second and the third telecommunication windows located at 1310 and at 1550 nm respectively [1]. The main factor limiting the development of these devices is the propagation losses. A composition based on an ormosil, 3-trimethoxysilylpropylmethacrylate [MAPTMS], has already allowed the industrial fabrication of optical integrated devices functioning at 1310 nm. At this wavelength, losses are 1 dB/cm. However, at 1550 nm, attenuation are too high (3 dB/cm) for the fabrication of efficient optical integrated devices or optical amplifiers via doping with rare earth ions [2–6]. Excited rare earth ions in solids can decay non-radiatively by multiphonon process when the number of phonon required to bridge the energy gap is less than four [6].

In organic and inorganic hybrids materials synthesised by the sol-gel process [7], attenuation at 1550 nm can be attributed to OH and CH groups which theoretically absorb in this spectral range and that are respectively inherent to the sol-gel process and to the precursor. The majority of previous works which aim at improving the transmission of hybrid materials in the near-infrared region call into question the absorption of OH groups [8–12]. This is the reason why many studies focused on the elaboration of OH free structures. A non-hydrolytic sol-gel process has been developed recently in order to synthesize hybrid oxide materials with low OH content [13, 14]. To activate the condensation reactions, this process requires high temperatures (generally higher than 500°C) and a neutral atmosphere during the synthesis. These drastic conditions imply damage to the organic part of the organically modified silicates, which is essential for the waveguide fabrication. Another study [15] showed the possibility to condense, at low temperature, a hybrid chlorosilane monomer via a non-hydrolytic sol-gel process. The use of 2-methyl-2-propanol, under vacuum, allows a breaking of the Si-Cl bond and induces the polycondensation reaction. More recently, a study [12] indicates the possibility to condense MAPTMS with diphenylsilane-

diol at high temperature with the use of a catalyst. Because of the organic part of the ormosil, we think that the treatment temperature can not exceed 120°C. Besides, the condensation reaction between methoxy and OH groups is possible via a classical sol-gel reaction implying the formation of a siloxane bond and elimination of methanol. The performances indicated for the waveguide prepared from this material are: 0.3 and 0.6 dB/cm respectively at 1310 nm and at 1550 nm. These values, attributed to the low OH content in the material, are in agreement with our previous conclusions [16] but remain surprising due to the high CH content [15]. Thus it is necessary to highlight the molecular groups responsible for the attenuation at the desired wavelengths.

This study involves a well known composition obtained by hydrolysis of a mixture of pre-hydrolyzed MAPTMS and the complex issued from the chelation of the zirconium (IV) *n*-propoxide by the methacrylic acid. A previous structural characterization [16] has indicated remaining ZrOH groups in the final material which is the consequence of a partial condensation during gelation and heat treatment. On the basis of the assumption that ZrOH groups are indeed responsible for the attenuation at 1550 nm, the objective of this work is to decrease their concentration in the sol in order to eliminate them in the final material and to allow a discussion on the contribution of each molecular group on the absorption at 1550 nm.

2. Experimental

2.1. Sol Preparation

The sol preparation, initiated by Krug [17], was based on the formation of a stable and homogeneous sol obtained by the mixture of a photosensitive organically modified silicate, MAPTMS (Assay ~99% in methanol), zirconium (IV) *n*-propoxide ($Zr(O_nC_3H_7)_4$), Assay ~70% in propanol) and methacrylic acid (MAAH, $C_4H_6O_2$, Assay >98%) in molar ratio of 2.5:1:1. All precursors were used without further purification. The difference of reactivity of each alcooxide implies a three-step process [16]. The pre-hydrolysis of the MAPTMS was followed by the addition of the complex issued from the chelation of $Zr(O_nC_3H_7)_4$ by MAAH and then a further hydrolysis of the mixture.

MAPTMS was hydrolysed with an aqueous solution with a 1:0.75 water to alcooxide ratio. As MAPTMS and

water were not miscible, the hydrolysis was performed in a heterogeneous way. After 20 min of stirring, the production of methanol became sufficient to allow the miscibility of all species present in solution. To control the hydrolysis condensation of $Zr(O_nC_3H_7)_4$, MAAH can covalently chelate the zirconium atom through two oxygen atoms. In our synthesis, MAAH was added dropwise to $Zr(O_nC_3H_7)_4$ with a molar ratio of 1:1, to form a modified zirconium alcoxide. A more detailed description of the reaction has been reported elsewhere [16].

2.2. Modification of the Initial Sol

To decrease the ZrOH concentration, we have decided to act on their condensation in the sol by catalysis or by reticulation. In this objective, hexamethyldisilazane [HMDSZ] and phosphorous derived: phenyl-phosphonic acid [$C_6H_7PO_3$, PA] and a bistrimethylsilyl-phosphonic ester [$C_6H_{23}PSi_2O_3$, PE] are good candidates. The N—H bond contained in HMDSZ is known [18] to be sensitive to OH groups. Then, it can act as a catalyst for the ZrOZr bonds formation. The phosphorus atom in PA and PE can directly react with ZrOH bond to form POZr bond. The stability of this bond has been already demonstrated [19]. The OH concentration has been followed by near infrared spectroscopy on bulks and by the evolution of the refractive index on coatings.

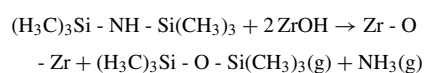
The resulting initial sol is modified by addition of HMDSZ, PA and PE in order to decrease the ZrOH concentration. They are added in solution in quantity to respect the fabrication protocol, which requires an optical quality coating. The compromise between these two conditions was found for concen-

tration less than 5% molar of the resulting material composition.

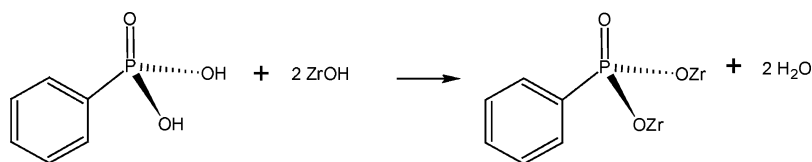
The addition of HMDSZ to the initial sol provokes spontaneously an ammoniac gaseous emission and an increase of the viscosity of the sol. This is the consequence of a formation of a higher condensed macromolecular system due to the increase of the ZrOZr bonds (Scheme 1). As for HMDSZ, the addition of PA or PE provokes spontaneously an increase of the viscosity of the sol. Moreover, a release of heat is observed showing the formation of a more stable structure. Then, to identify the effect of the phosphonates groups, we followed the chemical reaction with ^{31}P -NMR spectroscopy. In both cases, we observed the same spectrum up to 24 h of reaction (Fig. 1). This result demonstrates that PA and PE react in the same way with the initial sol. Moreover, the total disappearance of the PA and PE peaks, respectively located at 2.1 and 1.6 ppm indicates a total reaction with the sol.

However, similar ^{31}P -NMR spectra have been recorded for closed materials [20–23]. The numerous peaks observed were identified to be originating from both the normal and the tridentate character of the phosphorus atom which can induce several kinds of oligomers structures: linear, cyclic and polycyclic [23]. On this basis, we can assign all the observed peaks (Table 1) and describe the associated chemical reactions (Schemes 2 and 3).

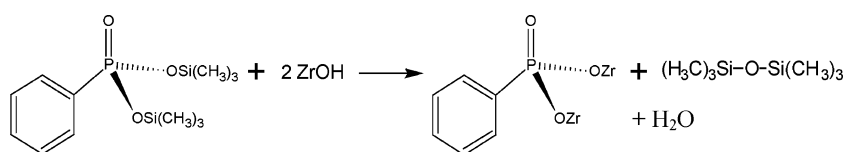
For practical reasons, only one ZrOH bond was represented on zirconium atom. Its normal valence (four) is assured by MAAH and propoxide or another OH group.



Scheme 1.



Scheme 2.



Scheme 3.

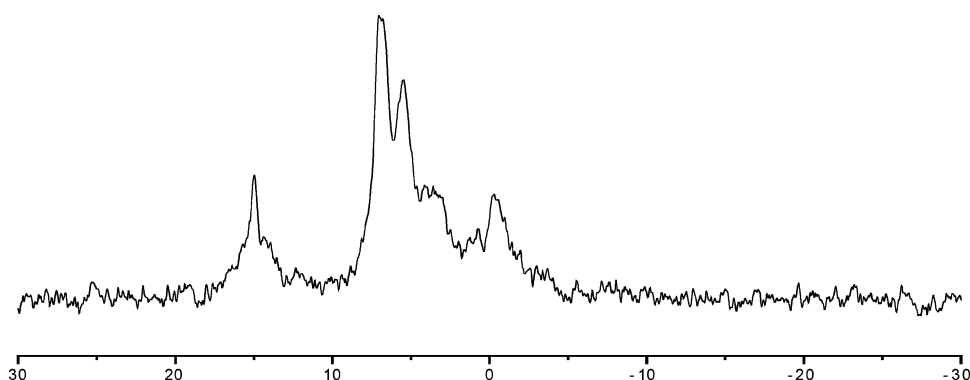


Figure 1. ^{31}P -NMR spectrum of the initial sol modified with PA or PE.

3. Results and Discussion

3.1. ^{29}Si NMR Spectroscopy

Spectrum obtained on liquid solution was measured at room temperature. Accumulation parameters are presented in Table 2. The signal chemical shift reference was tetramethylsilane (TMS). The FID processing used a 10 Hz line broadening.

^{29}Si NMR spectroscopy is a convenient technique to follow the various oxobridges formed during a siloxane hybrid network synthesis and to identify the interaction between various minerals networks in growth [24]. It can also be used as a technique for the analysis of alcoxide purity.

^{29}Si NMR spectrum of the pure MAPTMS alcoxide (not shown) presents a single peak at -42.8 ppm demonstrating the absence of any hydrolysed or condensed species. Such species are indeed expected

Table 1. Assignments of ^{31}P -NMR signals for monomeric and oligomeric species obtained from the modification of the initial sol with PA and PE.

Chemical shift (ppm)	Assignments
-0.4	$\text{PhP}(\text{OZr})_3$
$3.6; 5.5; 6.7; 6.9$	$\text{PhPO}(\text{OZr})_2$ cyclic or polycyclic oligomers
15	$\text{PhPO}(\text{OZr})_2$ linear oligomers

Table 2. Experimental acquisition conditions for ^{29}Si NMR spectroscopy.

State	Frequency (MHz)	Recycle delay (s)	Pulse	Spectral width (ppm)	Scans
Liquid	46.69	4	$\pi/3$ ($8 \mu\text{s}$)	500	80

at lowers chemicals shifts as shown previously in the same structure [16] and in analogous structures [25–29].

This result proves the high purity and stability of the used precursor. Humidity of ambient air is not sufficient to hydrolyse MAPTMS. This is not the case of zirconium, titanium and aluminium alcoxide which precipitates spontaneously and need a preable chelation with strong complexing ligand in order to control hydrolysis condensation reactions [30].

3.2. Near Infrared Spectroscopy

The transmission spectra of the samples were taken using a near infrared spectrometer. This optical spectrum analyzer included an infrared source, a second order blocking filter and a scanning monochromator (Ge(1) or PbSe(2)). The system 1 (Ge) was optimised in the range 600–1900 nm and the system 2 (PbSe) between 1500 and 3000 nm. The resolution can be chosen between 0.25 and 20 nm. The scanning monochromator used a continuously rotating diffraction grating driven by an electronically controlled DC motor. Except for MAPTMS, all spectra were measured on monolithic samples to which thickness were close to 5 millimetres.

Near infrared spectroscopy enables to localize the absorption of the harmonics bands and the combinations of the fundamental vibrations in the middle infrared region.

Figure 2 presents spectrum obtained in the near infrared region for MAPTMS. It is essentially composed of four bands located at 1200, 1400, 1630 and 1725 nm. As the presence of SiOH groups has been excluded by ^{29}Si NMR spectroscopy, all the bands are attributed to

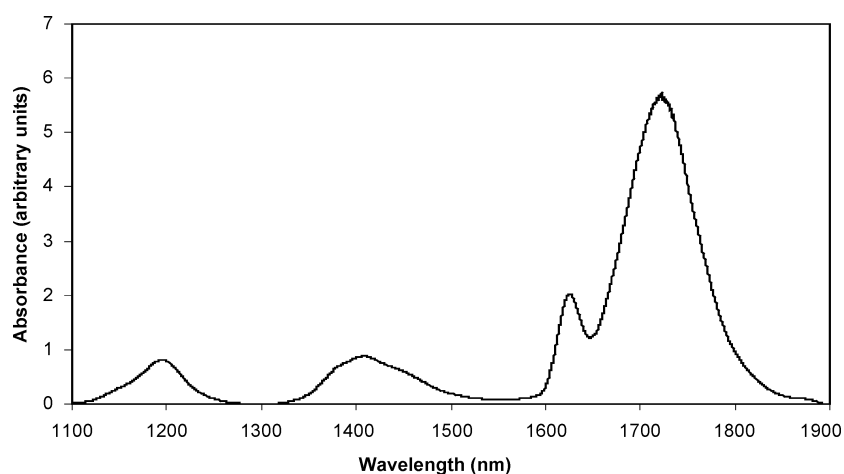


Figure 2. Near infrared spectrum of pure liquid MAPTMS.

the organic host in Table 3. This assignment is in good agreement with previous works [31].

The band centred at 1725 nm correspond to the first harmonic of CH bonds contained in CH_3 and CH_2 saturated groups. CH_3 groups are both linked to an oxygen atom, in the alcoxide function, and to a carbon atom, in the methacrylate function. CH_2 saturated groups are essentially positioned in the aliphatic propyl chain which connects the two ends of the molecule. Finally five environments are determined for CH aliphatic bonds in CH_3 and CH_2 which explain the important broadening (about 95 nm) of the band centered at 1725 nm which results from combination of CH fundamental modes. The band centered at 1630 nm correspond to the first harmonic linked to the vinylic CH groups. Its weak width (20 nm) is due to the single configuration of the unsaturated CH groups in MAPTMS. On the other hand, the large band positioned between 1380 and 1450 nm is due to the many combinations possibles between the first harmonics and the bending of the CH aliphatics groups. In the same spectral range, combinations between the first harmonic of CH groups and the fun-

damental vibrations of the mineral network contribute to the broadening of the band. At 1200 nm, the second harmonics of CH aliphatics groups is located. It is finer and less intense than the first harmonic since it requires a three order process which probability is weaker than a two order process.

Transmissions for the second and the third telecommunication windows are respectively of 100 and 92%. There is thus no contribution of the CH absorption at 1300 nm. On the other hand, at 1550 nm, there is a probable contribution of aliphatic or vinylic CH absorption. To precise their respective contributions, it is necessary to make a theoretical study based on the decomposition of all the bands. The technique of decomposition used here has been already described [32].

The modelling of the spectrum of the MAPTMS by gaussian functions shows the combinations of many absorptions bands for the reconstitution of the bands centred at 1200, 1400, 1630 and 1725 nm (Fig. 3) and reveals existence of two bands localized at 1587 nm (6300 cm^{-1}) and at 1515 nm (6600 cm^{-1}) who are responsible for the absorptions at 1550 nm. Then a more precise attribution of all the absorptions bands has been realized (Table 4).

Although these measurements were carried out on the liquid precursor, the highlighted absorptions bands will be found in the solid final material. Their contribution near that of OH groups is then certain to the total attenuation. This result indicates that a free OH system shows inherent absorptions around 1550 nm, linked to the organic precursor. Consequently, it will be necessary to minimize the concentration of CH aliphatic groups.

Table 3. Attribution of the absorptions bands of the experimental MAPTMS spectrum.

Wavelength (nm)	Assignments
1200	$3\nu \text{ CH} [\text{CH}_3 \text{ ou } \text{CH}_2]$
1380–1450	$2\nu \text{ CH} [\text{CH}_3] + \delta \text{ CH} [\text{CH}_3 \text{ or } \text{CH}_2]$
	$2\nu \text{ CH} [\text{CH}_3] + \nu \text{ SiOCH}_3$
1630	$2\nu \text{ CH} [\text{CH}=\text{CH}]$
1680–1750	$2\nu \text{ CH} [\text{CH}_3 \text{ ou } \text{CH}_2]$

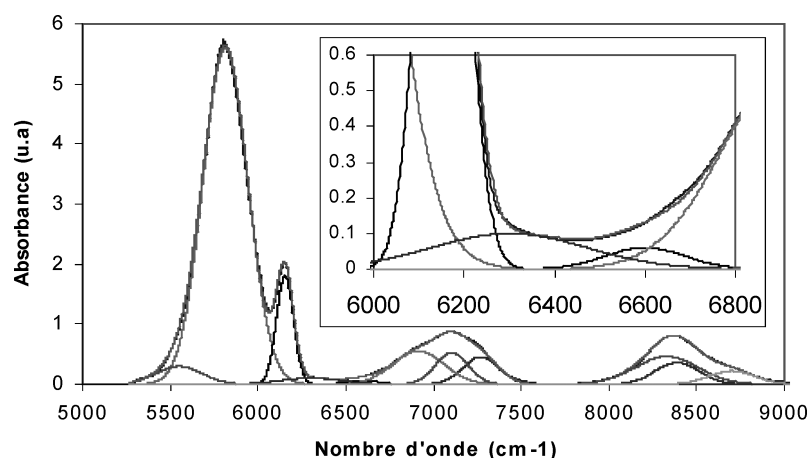


Figure 3. Decomposition of the near infrared spectrum of pure liquid MAPTMS, by gaussian lines.

The near infrared spectra issued from the material modified respectively with HMDSZ, PA and PE do not show any difference with the initial spectrum (Fig. 3). The effect of the chemical modifiers, although obvious from a chemical point of view, does not modify the near infrared absorption spectra.

However, if the ZrOH concentration was effectively decreased, the refractive index should be decreased and then the optical characteristics affected. This is the purpose of the following refractometry analysis.

3.3. Refractometry

Refractometry is a convenient technique to determine the refractive index of coatings, which depend essen-

Table 4. Attribution of the absorptions bands of the theoretical MAPTMS spectrum.

Vibrations (cm ⁻¹)	Vibrations (nm)	Attributions
5550	1800	2νC—H [CH ₂ saturated or CH ₃]
5815	1719	2νC—H [CH ₂ saturated]
6154	1625	2νC—H [CH ₂ unsaturated]
6300	1587	2νC—H [CH ₂ ou CH ₃] + δC—C
6600	1515	2νC—H [CH ₂ ou CH ₃] + δC—O
7105	1407	2νC—H [CH ₂ ou CH ₃] + δC—H
7270	1375	2νC—H [CH ₂ ou CH ₃] + δC—H
6915	1446	2νC—H [CH ₂ ou CH ₃] + δC—H
8330	1200	3νC—H [CH ₂ saturated or CH ₃]
8390	1191	3νC—H [CH ₂ saturated]
8700	1149	3νC—H [CH ₂ saturated]

tially on chemical and physical parameters such as composition and heat treatment densification. Refractive indexes of all coatings have been measured with an Abbe refractometer in the visible (632.8 nm).

Figure 4 shows the evolution of the refractive index of coatings, sintered ten min at 60°C and UV photo-cured during 90 sec, as a function of the composition MAPTMS/Zr(OC₃H₇)₄/MAA:10/X/X. Refractive index varies from 1.502, for pure MAPTMS, to 1.532, for the higher zirconate concentration (10/4.5/4.5 composition). The initial zirconate contribution provokes an increase of 33% of the total increase induced by the 10/4.5/4.5 composition which is nine times more concentrated. Contrary to pure mineral materials, this refractive index behavior is not following a classical law of mixing [33, 34]. A similar behavior has been already observed [34] for organic and inorganic hybrids materials and can constitute a specificity of these materials.

If one neglects the pure MAPTMS refractive index, the curves becomes linear, represented by the linear regression indicated by dotted lines. The non linear behavior can be explained by the transition from a simple to a mixed oxide. Initially, only the silicon atom has the vocation to form the three-dimensional network. The zirconate introduction induces a reorganization of the roles. It becomes the principal agent of gelation. As soon as the system becomes mixed, the linear increase depends on the regular zirconate content of which its high atomic size and its strong polarizability provoke a more important molar refraction.

Results indicated by Krug [15] reveal a linear behavior and lower refractive index values for all

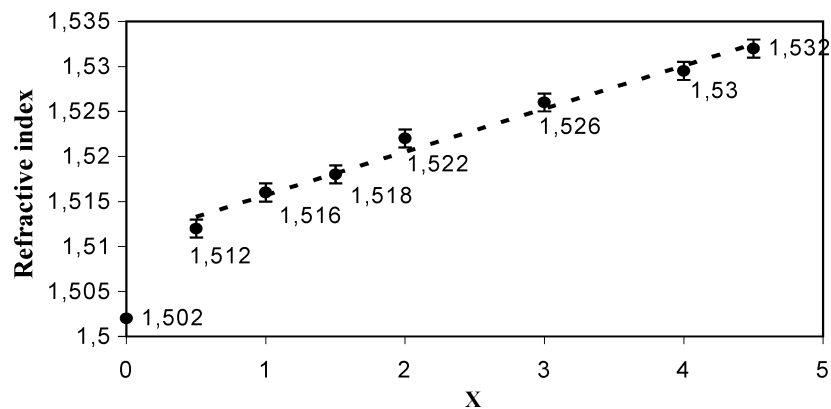


Figure 4. Refractive index of 10/X/X (MAPTMS/Zr(O_nC₃H₇)₄/MAA) compositions.

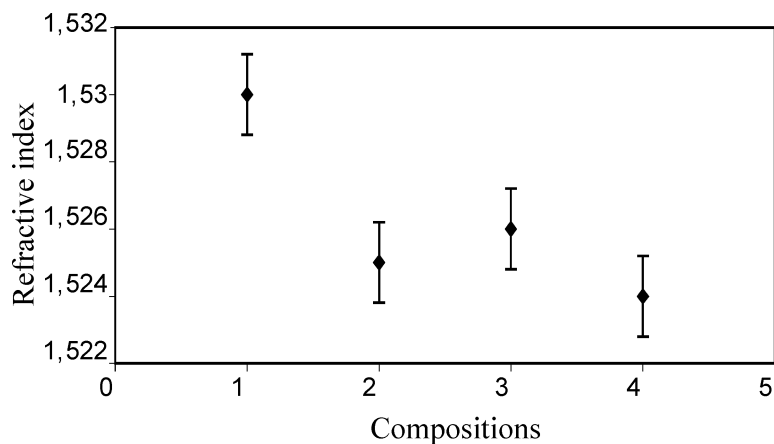


Figure 5. Refractive index of the 10/4/4 coating (1) modified by HMDSZ (2), PA (3) and PE (4).

concentrations. This is due probably to the higher heat treatment (one hour at 130°C) imposed to the coatings, which increase the network connexity by an increase in the ZrOH bonds condensation rate. The consequence is then a decrease in the total molar refraction traduced by a decrease of the refractive index.

Figure 5 shows the refractive index values for the different 10/4/4 modified composition. In general, compared to the initial material, one can observe a decrease of about 5 to 7 thousandths. This reproducible result proves a real modification on the morphology of the material since it traduces an effect on the average molar refraction or on the density or both. However, the difficulty to measure the density of the resulting bulks cannot permit us to separate the mentioned hypothesis.

On the basis of ³¹P-NMR results, which demonstrated an effective condensation of the ZrOH groups,

and by analogy with preceding results on similar materials [35], we can suggest that the reaction of PA and PE on the initial sol does not increase the density. Hence, the observed phenomenon is a consequence of a decrease of the average molar refraction. Indeed, it is well known that the molar refraction of a hydroxyl group is higher than its analogue oxide [35].

4. Conclusion

Through the spectroscopic and optical study of a reference organic and inorganic hybrid material, in this paper, we have highlighted the chemical groups responsible for the attenuation at the third telecommunication window. Near infrared spectroscopy revealed the existence of absorption at 1550 nm in a free OH precursor. The theoretical study of the various near infrared

spectrum absorption bands showed the responsibility of CH aliphatic groups at 1550 nm. Various chemical treatments imposed to the final material in order to reduce the OH concentration have not permitted to improve transmission at 1550 nm.

The whole of these results shows that the measured attenuation at 1550 nm are ascribable to the organic network. The excellent performances indicated in the literature and attributed to the absence of OH groups are probably linked to the decrease in the aliphatic CH groups concentration for the benefit of aromatic CH groups, which absorption is probably lower at 1550 nm. Their respective contribution will be discussed in further studies.

References

1. P. Coudray, P. Etienne, and Y. Moreau, *J. Porque, Opt. Comm.* **143**(4–6), 199 (1997).
2. B.T. Stone and K.L. Bray, *J. Non-Cryst. Solids* **197**, 136 (1996).
3. Y. Zhou, Y.L. Lam, S.S. Wang, H.L. Liu, C.H. Kam, and Y.C. Chan, *Appl. Phys. Lett.* **71**, 587 (1997).
4. C. Strohhofer, S. Capecci, J. Fick, A. Martucci, G. Brusatin, and M. Guglielmi, *Thin Solid Films* **326**, 99 (1998).
5. E.M. Yeatman, M.M. Ahmad, O. McCarty, A. Vannucci, P. Gastaldo, D. Barbier, D. Mongardien, and C. Moronvalle, *Opt. Comm.* **164**, 19 (1999).
6. C.B. Layne, W.H. Lowdermilk, and M.J. Weber, *Phys. Rev. B* **16**, 10 (1977).
7. C.J. Brinker and G.W. Scherrer, *Sol-Gel Science* (Academic Press, San Diego, CA, 1990).
8. P. Coudray, P. Etienne, and Y. Moreau, *Mater. Sci. Semicond. Proc.* **3**(5/6), 331 (2000).
9. P. Etienne, P. Coudray, J. Porque, and Y. Moreau, *Opt. Mat.* **174**(5/6), 413 (2000).
10. M. Popall, R. Buestrich, F. Kahlenberg, A. Adersson, J. Haglund, M.E. Robertsson, G. Blau, M. Gale, O. Rösch, A. Dabek, J. Neumann-Rodekirch, L. Cergel, and D. Lambert, *Mater. Res. Soc. Symp. Proc.* **628**, CC9.8.1 (2000).
11. M. Popall, A. Dabek, M.E. Robertsson, S. Valizadeh, O.J. Hagel, R. Buestrich, R. Nagel, L. Cergel, D. Lambert, and M. Schaub, *Mol. Cryst.* **354**, 123 (2000).
12. R. Buestrich, F. Kahlenberg, M. Popall, P. Dannberg, R. Müller-Fiedler, and O. Rösch, *J. Sol-Gel Sci. Technol.* **20**, 181 (2001).
13. A. Vioux, *Chem. Mater* **9**, 2292 (1997).
14. R. Buestrich, F. Kahlenberg, M. Popall, A. Martin, and O. Rösch, *Mater. Res. Soc. Symp. Proc.* **628**, CC 9.8.1 (2000).
15. M. Mennig, M. Zahnhausen, and H. Schmidt, *Proc. SPIE* **3469**, 68 (1998).
16. M. Oubaha, M. Smaïhi, P. Etienne, P. Coudray, and Y. Moreau, *J. Non-Cryst. Solids* **318**, 305 (2003).
17. H. Krug, F. Teillant, P.W. Oliviers, and H. Schmidt, *Proc. SPIE* **1758**, 448 (1992).
18. M.G. Fonseca, A.S. Oliveira, and C. Airoidi, *J. Colloid Interf. Sci.* **240**(2), 533 (2001).
19. R.L. Ballard, J.P. Williams, J.M. Njus, B.R. Kiland, and M.D. Soucek, *Europ. Polym. J.* **37**(2), 381 (2001).
20. P.H. Mutin, G. Guerrero, and A. Vioux, *C.R. Chimie* **6**, 1153 (2003).
21. G. Guerrero, P.H. Mutin, and A. Vioux, *J. Mater. Chem.* **3161** (2001).
22. G. Guerrero, P.H. Mutin, and A. Vioux, *Chem. Mater.* **12**(5), 1268 (2000).
23. G. Guerrero, PhD Thesis, Montpellier, 2000.
24. H. Marsmann, *Oxygen-17 and Silicon-29 NMR Spectroscopy* (Springer, Berlin, 1981).
25. T. Jermoumi, M. Smaïhi, and N. Hovnanian, *J. Mater. Chem.* **5**(8), 1203 (1995).
26. Y. Sugahara, S. Okada, S. Sato, K. Kuroda, and C. Kato, *J. Non-Cryst. Solids* **167**, 21 (1994).
27. Y. Sugahara, S. Okada, S. Sato, K. Kuroda, and C. Kato, *J. Non-Cryst. Solids* **139**, 25 (1992).
28. L. Bois, PhD Thesis, Paris VI, 1993.
29. F. Babonneau, and J. Maquet, *Polyhedron* **19**, 315 (2000).
30. J. Livage and C. Sanchez, *J. Non-Cryst. Solids* **145**, 11 (1992).
31. D. Li Ou and A.B. Seddon, *J. Non-Cryst. Solids*, **210**, 187. (1997)
32. S. Calas, PhD Thesis, Montpellier, 1997.
33. H. Shroeder, *Physics of Thin Solid Films* (Academic Press, N.Y.5, 87, 1969).
34. F. Bissuel, PhD Thesis, Montpellier, 1996.
35. M.C. Gonçalves and R.M. Almeida, *J. Non-Cryst. Solids* **194**, 180 (1996).